Article published online: 2022-07-07

Effects of Gancao Nourish-Yin Decoction on Liver Metabolic Profiles in hTNF-α Transgenic Arthritic Model Mice

Rongbin Pan[1] Kok Suen Cheng[1,2] Yanjuan Chen[3] Xingwang Zhu[4] Wenting Zhao[4] Changhong Xiao[4] Yong Chen[5]

[1] Jiangzhong Cancer Research Center, Jiangxi University of Chinese Medicine, Nanchang, Jiangxi, China
[2] College of Engineering, Peking University, Beijing, China
[3] School of Medicine, Ji'nan University, Guangzhou, Guangdong, China
[4] Department of Immunology and Rheumatology, Integrative Hospital of Traditional Chinese Medicine, Southern Medical University, Guangzhou, Guangdong, China
[5] Department of Rheumatology and Immunology, Shenzhen People's Hospital (The Second Clinical Medical College, Ji'nan University, The First Hospital Affiliated to Southern University of Science and Technology), Shenzhen, Guangdong, China

Address for correspondence Yong Chen, Associate Researcher, Department of Rheumatology and Immunology, Shenzhen People's Hospital, 1017 Dongmen North Road, Luohu District, Shenzhen, Guangdong 518020, China (e-mail: sgcy88888888@qq.com).

CMNP 2022;2:e19–e27.

Abstract

Objective *Gancao Nourish-Yin Decoction* (GNYD) has been applied to clinical rheumatoid arthritis (RA) patients, and it had shown effectiveness not only in disease activity controlling but also in improving patients' physical status. However, its mechanism of function has not been investigated. Metabolic perturbations have been associated with RA, and targeting the metabolic profile is one of the ways to manage the disease. The aim of this study is to observe the effect of GNYD on metabolic changes of human tumor necrosis factor α (hTNF-α) transgenic arthritic model mice.

Methods hTNF-α transgenic arthritic model mice were divided into the control group and the GNYD group with six mice in each group. After 8 weeks of treatment, liver tissues of mice in both groups were obtained for liquid chromatography-mass spectrometry analysis. Significantly regulated metabolites by GNYD treatment were first identified, followed by Kyoto Encyclopedia of Genes and Genomes pathway and network analysis.

Results A total of 126 metabolites were detected in the liver. Compared with the control group, 17 metabolites in the GNYD group were significantly altered. Specifically, thiamine, gamma-L-glutamyl-L-valine, pantothenic acid, pyridoxal (vitamin B6), succinic acid, uridine 5′-diphospho-glucuronic acid, uridine, allantoic acid, N-acetyl-D-

Keywords
- rheumatoid arthritis
- Gancao Nourish-Yin Decoction
- hTNF-α
- liver metabolism
- metabolomics

The study protocol of the animal experiments was approved by the Ethics Committee of integrative Traditional Chinese and Western Medicine Hospital, Southern Medical University, China (approval No. NFZXYEC-2017-002).

received
November 24, 2021
accepted after revision
January 23, 2022

DOI https://doi.org/10.1055/s-0042-1747916.
ISSN 2096-918X.

Georg Thieme Verlag KG, Rüdigerstraße 14, 70469 Stuttgart, Germany

glucosamine, nicotinamide ribotide, and N2, N2-dimethylguanosine were down-regulated by GNYD treatment, whereas isobutyrylglycine, N-acetylcadaverine, N-carbamoyl-L-aspartic acid, L-anserine, creatinine, and cis-4-hydroxy-D-proline were up-regulated. Six metabolic pathways were significantly altered including the alanine, aspartate, and glutamate metabolism; pyrimidine metabolism; thiamine metabolism; amino sugar and nucleotide sugar metabolism; pantothenate and CoA biosynthesis; and citrate cycle. Integrative metabolic network analysis suggested the possibility of GNYD having both positive and negative effects on RA through the suppression of angiogenesis and the promotion of leukocyte extravasation into the synovium, respectively.

Conclusions GNYD can modulate the hepatic metabolism of hTNF-α transgenic arthritic model mice. Further optimization of this decoction may lead to better therapeutic effects on RA patients.

Introduction

Rheumatoid arthritis (RA) is a chronic autoimmune disease, which is responsible for progressive articular damage, functional loss of joints, and comorbidity.[1] Treatment for RA has changed profoundly over the past decades, but modern medicine still lacks in terms of symptom relief and mending joint structural damage.[2] RA in traditional Chinese medicine (TCM) is known as Bi that is the physical pain or numbness caused by wind, cold, and humidity that can cause the stagnation of qi and blood stasis.[3] Multiple TCM treatment methods including acupuncture, moxibustion, and herbal medicine have been applied as complementary management of RA, and many effective benefits have been reported.[4,5] Among the plethora of herbal medicine available, *Gancao Nourish-Yin Decoction* (GNYD) can be an effective complementary medicine for RA. GNYD is a herbal formula developed from *Essentials from the Golden Cabinet(Jin Gui Yao Lüe)*, which is a classical medical book authored by Zhongjing Zhang during the Han dynasty (AD. 150–154). The formula was associated with acute or chronic gastrointestinal inflammation and Huhuo disease (similar to Behcet's syndrome, an autoimmune disorder).[6] Although its constituents such as Gancao (glycyrrhizae),[7] Renshen (ginseng),[8] Ganjiang (ginger),[9] and others were reported to be anti-inflammatory by an abundance of research, little is known about the integrative mechanism of the formula that will be more of significance from a clinical perspective.

Many pieces of evidence suggest that cellular metabolic alterations fuel and dictate the inflammatory state of cells. Data from RA patients demonstrated a strong link between the degree of systemic inflammation and the development of insulin resistance.[10] The induction of arthritis in mice resulted in a global inflammatory state that is characterized by defective carbohydrate and lipid metabolism in different tissues.[11] Therapeutic strategies based on tighter control of inflammation provide promising approaches to normalize and prevent metabolic alterations associated with RA.[12]

For animal models of RA, human tumor necrosis factor α (hTNF-α) mimics human RA clinical presentations including polyarticular swelling, impairment of movement, synovial hyperplasia, and cartilage and bone erosion.[13] The systematical and joint manifestations are stable and have been applied in metabolic research studies.[14] In this study, we investigate the effects of GNYD on the metabolic profiles of hTNF-α transgenic arthritic model mice.

Materials and Methods

Animals and Grouping

hTNF-α transgenic arthritic model mice [CAS: SCXK (Guangdong) 2018-0044] were bought from Guangdong Experimental Animal Monitoring Institute, China. The transgenic mouse line was produced by using a hTNF/β-globin (TNF-globin) recombinant gene construct that contained a 2.8 kb fragment of the entire coding region and promoter of the hTNF-α gene fused to a 0.77 kb fragment of 3′ untranslated region and polyadenylation site of human β-globin replacing that of the hTNF-α gene. The fragment was then microinjected into the pronuclei of FVB/J inbred strain fertilized eggs that were subsequently implanted into the fallopian tube of 8-week-old female pseudo-pregnant ICR mice. Transgenic lineages were established by backcrossing the transgenic founder individuals to the FVB/J inbred strain.[13]

The hTNF-α transgenic arthritic model mice at 16 weeks of age (SPF grade, all males, 28–33 g) were divided into the control group and the GNYD group with six mice in each group after 1 week of adaptive feeding. The GNYD group was treated with GNYD (CAS: 20200601, provided by Qianzheng Health Technology Development Co., Ltd. Shanghai, China) with free access to drinking water (equivalent to 6.3 times the amount of a 60 kg adult), whereas the control group mice were fed with routine water supply. The temperature of the breeding environment for the mice was kept at 26°C, and the relative humidity was 60%. The treatment lasted for 8 weeks. Then, the mice were put into anesthesia by intramuscular injection of Zoletil 50 (Virbac, France), and liver tissues were collected into biopsy boxes. Mice were euthanized by cervical dislocation.

Liquid Chromatography-Mass Spectrometry-Based Metabolomics

Twenty-five milligrams of liver tissue sample was weighed into a centrifuge tube, and 500 µL of extract solution (acetonitrile: methanol: water = 2: 2:1) was added. After 30 s of vortex, the samples were homogenized at 35 Hz for 4 minutes and sonicated for 5 minutes in an ice-water bath. The homogenization and sonication cycle was repeated three times. Then, the samples were incubated at −40°C. Four hundred microliter of supernatant was transferred to a fresh tube and dried in a vacuum concentrator at 37°C. Next, the dried samples were reconstituted in 100 µL of 50% acetonitrile by sonication on ice for 10 minutes. The constitution was then centrifuged at 12 000 rpm·min^{-1} for 15 minutes at 4°C, and 75 µL of the supernatant was transferred to a fresh glass vial for liquid chromatography-mass spectrometry analysis. The quality control sample was prepared by mixing an equal volume of aliquots of the supernatants from all of the samples.

The ultra-high-performance liquid chromatography (UHPLC) separation was performed using an Agilent 1290 Infinity series UHPLC System (Agilent Technologies) equipped with a UPLC BEH Amide column (2.1 × 100 mm, 1.7 µm, Waters). The mobile phase consisted of 25 mmol • L^{-1} ammonium acetate and 25 nmol• L^{-1} ammonia hydroxide in water (pH = 9.75) (solution A) and acetonitrile (solution B). The elution gradient was set as follows: 0 to 1.0 minute, 95% solution B; 1.0 to 14.0 minutes, 95 to 65% solution B; 14.0 to 16.0 minutes, 65 to 40% solution B; 16.0 to 18.0 minutes, 40% solution B; 18.0 to 18.1 minutes, 40 to 95% solution B; and 18.1 to 23.0 minutes, 95% solution B. The flow rate was 0.5 mL• min^{-1}, whereas the column temperature was 25°C. The autosampler temperature was 4°C, and the injection volume was 2 µL (positive) or 2 µL (negative). An Agilent 6495 triple quadrupole mass spectrometer (Agilent Technologies) was applied for the assay development, and the parameters were as follows: capillary voltage = +3,000/− 2,500 V, N_2 temperature = 170°C, N_2 flow rate = 16 L• min^{-1}, sheath gas

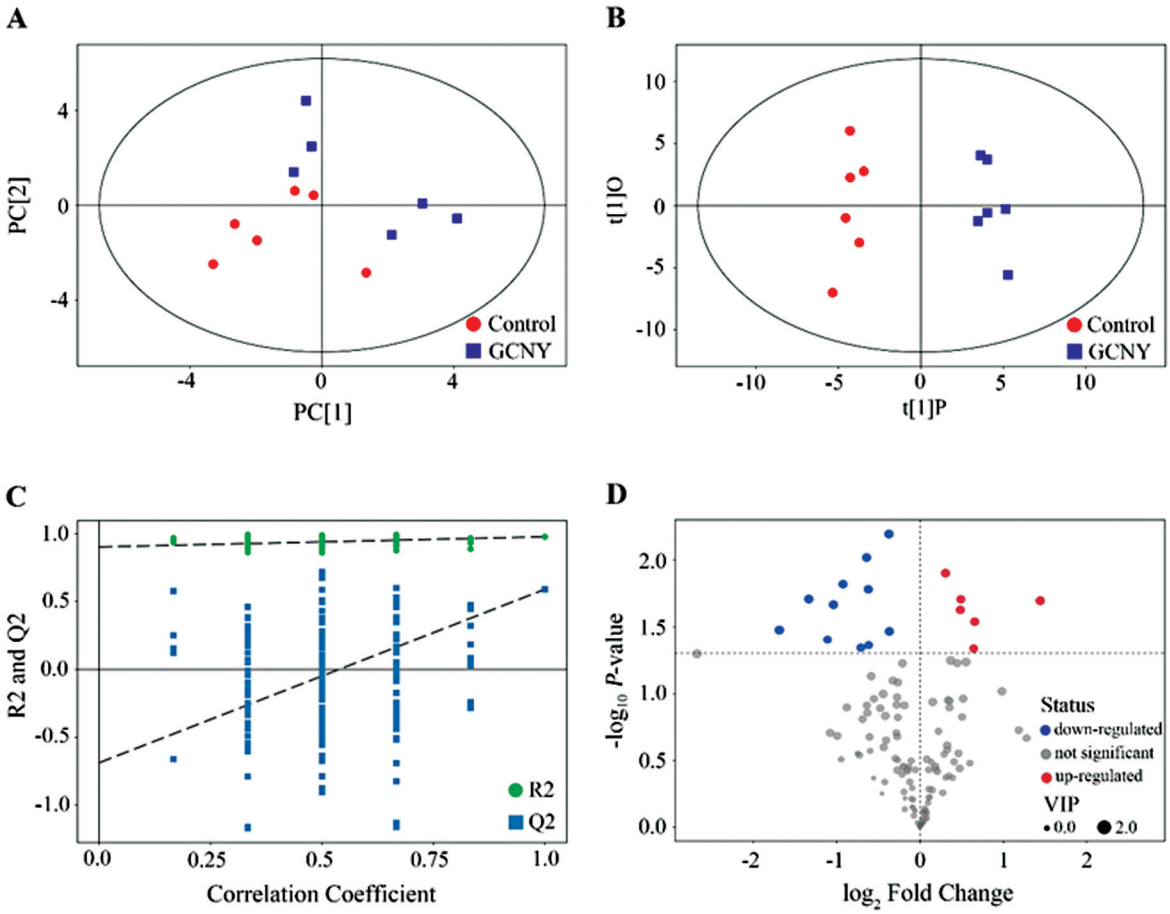

Fig. 1 *Multivariate analyses of metabolite signatures and identification of significantly regulated metabolites.* (**A**) PCA score scatter plot of metabolite profiles in control mice and mice treated with GNYD. Each point represents a metabolite profile of a biological replicate. All points fall within Hotelling's T2 ellipse (95% confidence interval). PC[1] and PC[2]: principal component 1 and 2. (**B**) OPLS-DA score scatter plot of metabolite profiles in control mice and mice treated with GNYD. R^2X, R^2Y, and Q^2 were 0.332, 0.977, and 0.590, respectively. Each point represents a metabolite profile of a biological replicate. All points fall within Hotelling's T2 ellipse (95% confidence interval). t[1]P: predicted principal component score of the first principal component; t[2]O: orthogonal principal component score. (**C**) Validation of the OPLS-DA model using permutation test of 200 random permutations. Intercepts of R^2Y and Q^2 were (0, 0.9) and (0, −0.69), respectively. (**D**) Volcano plot identifying significantly regulated metabolites associated with GNYD treatment. A threshold of $p = 0.05$ ($-\log_{10} p = 1.3$) was used.

temperature = 350°C, sheath gas flow rate = 12 L• min^{-1}, nebulizer pressure = 40 psi, and fragmentor voltage = 380 V.

Preprocessing of Raw Data

Missing data in the raw data were first imputed by using the half minimum method.[15] Next, individual peaks with peak area >50% null and relative standard deviation >20% were removed.[16] Lastly, the normalization of the data was performed with respect to the total ion current.

Statistical Analysis

Statistical analysis was performed by using SIMCA v15.0.2 (Sartorius Stedium Data Analytics AB, Umea, Sweden). First, the data were preprocessed by multivariate analysis of principal component analysis (PCA) and orthogonal partial least squares discriminant analysis (OPLS-DA). The OPLS-DA model was verified by using a sevenfold cross-validation technique, and a permutation test (200 iterations) was performed to evaluate the fitting of the model.[17] The variable importance in the projection (VIP) score was calculated for each metabolite. Next, univariable *t*-test was used to compare the metabolite levels across the two groups. Hierarchical clustering was performed by calculating the Euclidean distance matrix and clustered by using the complete linkage method. Lastly, Pearson's correlation coefficient *r* was calculated for the difference of the metabolite levels between the two groups. $p < 0.05$ was considered statistically significant.

KEGG Pathway and Network Analysis

First, significantly regulated metabolites were annotated by using various databases such as the Human Metabolome Database (HMDB), Kyoto Encyclopedia of Genes and Genomes (KEGG), and Pubchem. After annotations, all the pathways that contain the significantly regulated metabolites were identified by using the *Mus musculus* KEGG pathway database. To reveal pathways that were highly correlated to GNYD treatment, enrichment analysis and topology analysis were performed to find the *p*-value and impact value, respectively. A pathway's impact value was evaluated as the total importance measures of the matched metabolites divided by the total importance measures of all metabolites in each pathway.[18]

Results

Identification of Significantly Regulated Metabolites

Preprocessing of the raw data revealed a total of 126 metabolites peaks. Unsupervised PCA showed almost total separation of clusters in the GNYD group and the control group with no outlier present (►**Fig. 1A**). ►**Fig. 1B** shows the supervised fitted model of OPLS-DA, and it can be seen that the separation of the two groups was much more distinct with an R^2X, R^2Y, and Q^2 of 0.332, 0.977, and 0.590, respectively, indicating that the model has good predictability.[19] After 200 permutations, the R^2Y and Q^2 values were generally lower than those of the original model and the Q^2 intercept value was <0 at (0, −0.69) (►**Fig. 1C**). These showed that there was no overfitting for the OPLS-DA model.[20,21] Based on the criteria of *T*-test, $p < 0.05$, and VIP > 1,[20,22] 6 significantly up-regulated and 11 significantly down-regulated metabolites were identified (►**Fig. 1D** and ►**Table 1**). Hierarchical clustering of the 17 significantly regulated metabolites

Table 1 Significantly regulated metabolites associated with GNYD treatment

Metabolite	Retention time (s)[a]	HMDB	Direction of regulation
Thiamine	625.69	HMDB00235	Down
gamma-L-Glutamyl-L-valine	719.42	HMDB11172	Down
Pantothenic acid	503.88	HMDB00210	Down
Pyridoxal (vitamin B6)	175.65	HMDB01545	Down
Succinic acid	742.40	HMDB00254	Down
Uridine 5′-diphospho-glucuronic acid (UDP-D-Glucuronate)	913.63	HMDB00935	Down
Uridine	282.02	HMDB00296	Down
Isobutyrylglycine	394.00	HMDB00730	Up
Allantoic acid	672.44	HMDB01209	Down
N-Acetylcadaverine	541.66	HMDB02284	Up
N-Acetyl-D-glucosamine	465.88	HMDB00215	Down
N-Carbamoyl-L-aspartic acid	805.11	HMDB00828	Up
Nicotinamide ribotide	884.74	HMDB00229	Down
N2,N2-Dimethylguanosine	338.43	HMDB04824	Down
L-Anserine	782.04	HMDB00194	Up
Creatinine	294.17	HMDB00562	Up
cis-4-Hydroxy-D-proline	665.11	HMDB60460	Up

Abbreviation: HMDB, human metabolome database.
[a]Median retention time.

further validated the specific up- or downregulatory effects of GNYD group as compared with the control group (►**Fig. 2A**).

Correlation Analysis of the Significantly Regulated Metabolites

►**Fig. 2B** shows the correlation analysis results of the 17 significant metabolites. A positive correlation was observed between metabolites regulated in the same direction, whereas an inverse correlation was always observed between metabolites regulated in opposite directions. Among the up-regulated metabolites, creatinine was positively correlated to both N-carbamoyl-L-aspartic acid and L-anserine ($r = 0.631$, $p = 0.028$ and $r = 0.810$, $p = 0.001$, respectively), whereas L-anserine was positively correlated to N-carbamoyl-L-aspartic acid ($r = 0.720$, $p = 0.008$). On the contrary, there was a significant positive correlation between down-regulated metabolites ($r > 0.8$), including gamma-L-Glutamyl-L-valine and uridine 5′-diphosphoglucuronic acid (UDP-D-Glucuronate) ($r = 0.859$, $p < 0.001$), pantothenic acid and uridine ($r = 0.835$, $p = 0.001$), pantothenic acid and UDP-D-Glucuronate ($r = 0.837$, $p = 0.001$), pantothenic acid and gamma-L-glutamyl-L-valine ($r = 0.969$, $p < 0.001$), succinic acid and nicotinamide ribotide ($r = 0.835$, $p = 0.001$), and L-anserine and creatinine ($r = 0.810$, $p = 0.040$). There was only one very strong

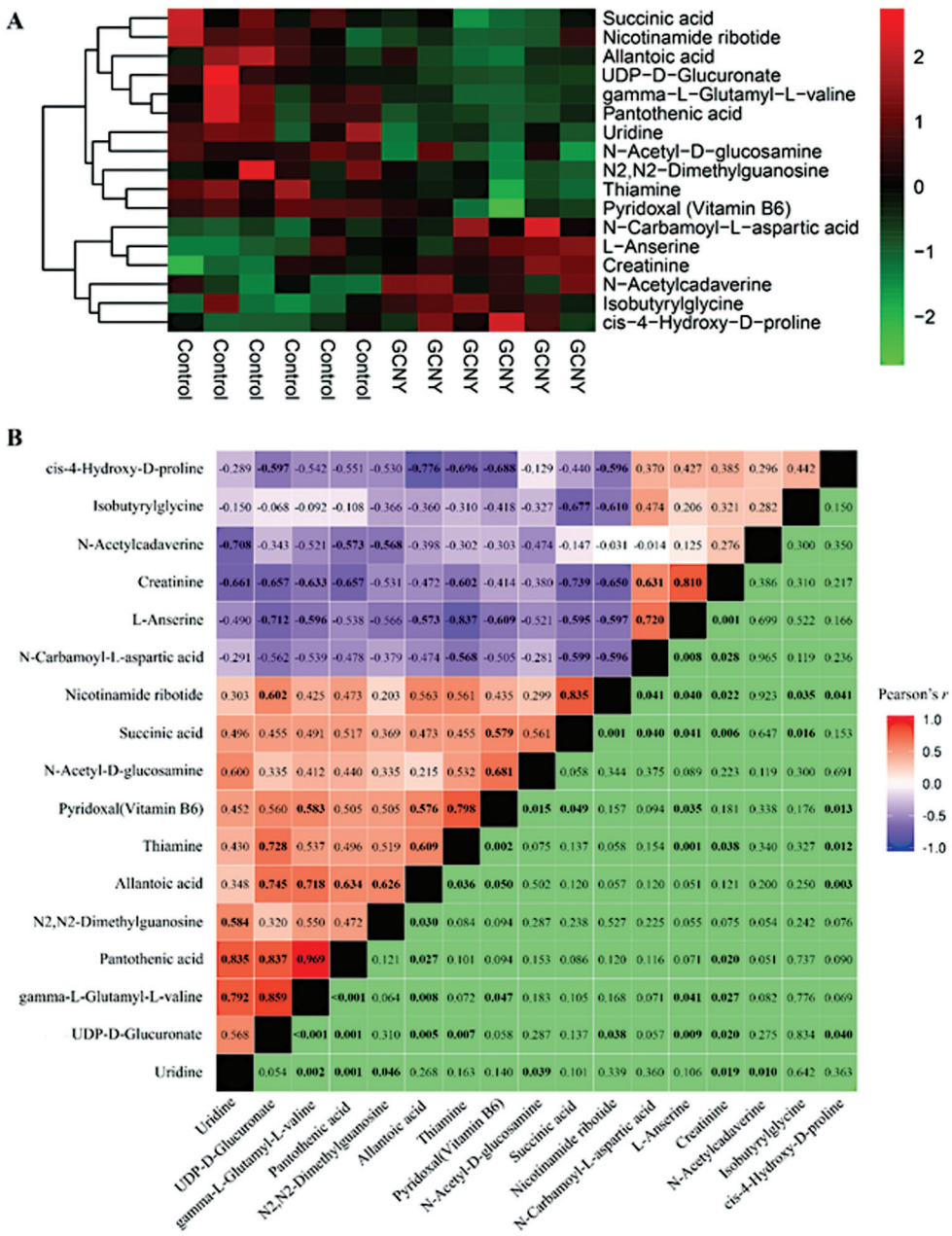

Fig. 2 *Analysis of significantly regulated metabolites.* (**A**) Hierarchical clustering analysis for the control group and the GNYD group. (**B**) Correlation analysis for the control group and the GNYD group. The upper triangle denotes Pearson's *r*, whereas the lower triangle denotes the respective *p*-values. Significant Pearson's *r* and *p*-values are bolded.

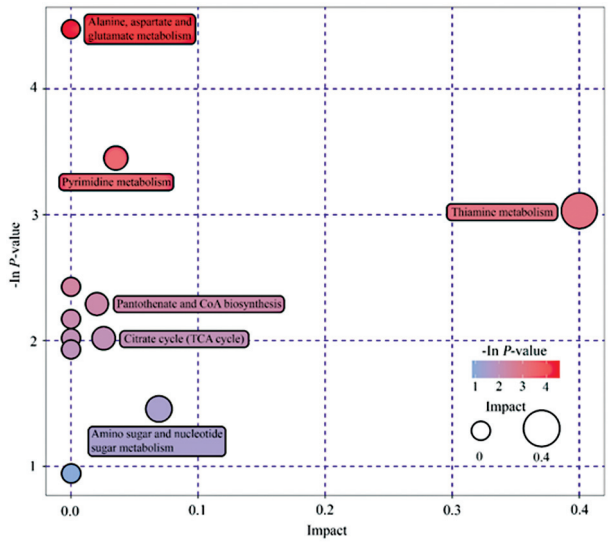

Fig. 3 *The metabolome view map of significantly altered pathways related to treatment with GNYD.* The *x*-axis represents the impact value in topology analysis, whereas the *y*-axis represents the *p*-value in enrichment analysis. Significantly altered pathways were labeled.

negative correlation ($r < -0.8$) observed for L-anserine and thiamine ($r = -0.837$, $p = 0.001$) (►**Fig. 2B**).

Metabolic Pathway and Integrative Network Analysis

Using the HMDB, Pubchem, and KEGG databases, all metabolic pathways involved in significantly regulating metabolites were identified and are shown in ►**Fig. S1**. Among these pathways, 11 metabolic pathways were associated with treatment by using GNYD (►**Fig. 3** and ►**Table 2**) with a high correlation. A combined consideration of the *p* and impact values revealed that six pathways were significantly altered: (1) alanine, aspartate, and glutamate metabolism; (2) pyrimidine metabolism; (3) thiamine metabolism; (4) amino sugar and nucleotide sugar metabolism; (5) pantothenate and CoA biosynthesis; (6) citrate cycle (TCA cycle). ►**Fig. 4** shows an integrative metabolic network that connected four of the six significantly altered pathways (pantothenate and CoA biosynthesis; pyrimidine metabolism; alanine, aspartate, and glutamate metabolism; and TCA cycle). Three metabolites, pantothenate, succinate, and uridine, were found to be down-regulated (fold change of 0.40, 0.53, and 0.64, respectively) following GNYD treatment, whereas only N-carbomoyl-L-aspartate, which was involved in both the alanine, aspartate, and glutamate metabolism and pyrimidine metabolism pathways, was found to be significantly up-regulated with a fold change of 2.72.

Discussion

The relationship between metabolism and inflammation has been profoundly investigated in recent decades. Although it is not yet known whether metabolic changes are a consequence of disease or whether primary changes to cellular metabolism might underlie or contribute to the pathogenesis of early-stage disease, changes to the metabolic profiles were observed in various diseases relating to inflammation and this includes RA as well.[23] Metabolic perturbations have been associated with RA whereby the hallmark swelling and heat observed in the joints of RA patients are considered to be a consequence of metabolic alterations. Daily whole-body resting energy expenditure is 8% higher in RA patients as compared with healthy individuals, and this suggests that these metabolic changes in RA are significant and systemic in nature.[23] Furthermore, the catabolic condition "cachexia" occurs in RA patients with muscle atrophy and increase in body fat is associated with systemically elevated levels of proinflammatory cytokines such as TNF, interleukin-1β (IL-1β), leukocyte inhibitory factor, interferon-γ, and IL-6.[23,24] Regulation on metabolism, for example, by inhibiting glucose metabolism exerted anti-inflammatory effects on

Table 2 Metabolic pathways associated with GNYD treatment

Pathway	Total[a]	Hits[b]	*p*-Value	Holm *P*[c]	Impact value
Alanine, aspartate, and glutamate metabolism	24	2	0.011	0.934	0.000
Pyrimidine metabolism	41	2	0.032	1.000	0.035
Thiamine metabolism	7	1	0.048	1.000	0.400
Nicotinate and nicotinamide metabolism	13	1	0.088	1.000	0.000
Pantothenate and CoA biosynthesis	15	1	0.101	1.000	0.020
β-Alanine metabolism	17	1	0.114	1.000	0.000
Propanoate metabolism	20	1	0.133	1.000	0.000
Citrate cycle (TCA cycle)	20	1	0.133	1.000	0.026
Butanoate metabolism	22	1	0.145	1.000	0.000
Amino sugar and nucleotide sugar metabolism	37	1	0.233	1.000	0.069
Purine metabolism	68	1	0.389	1.000	0.000

[a]Total metabolites in the pathway.
[b]Number of significantly regulated metabolites in the pathway.
[c]Holm–Bonferroni corrected *p*-values for multiple comparisons.

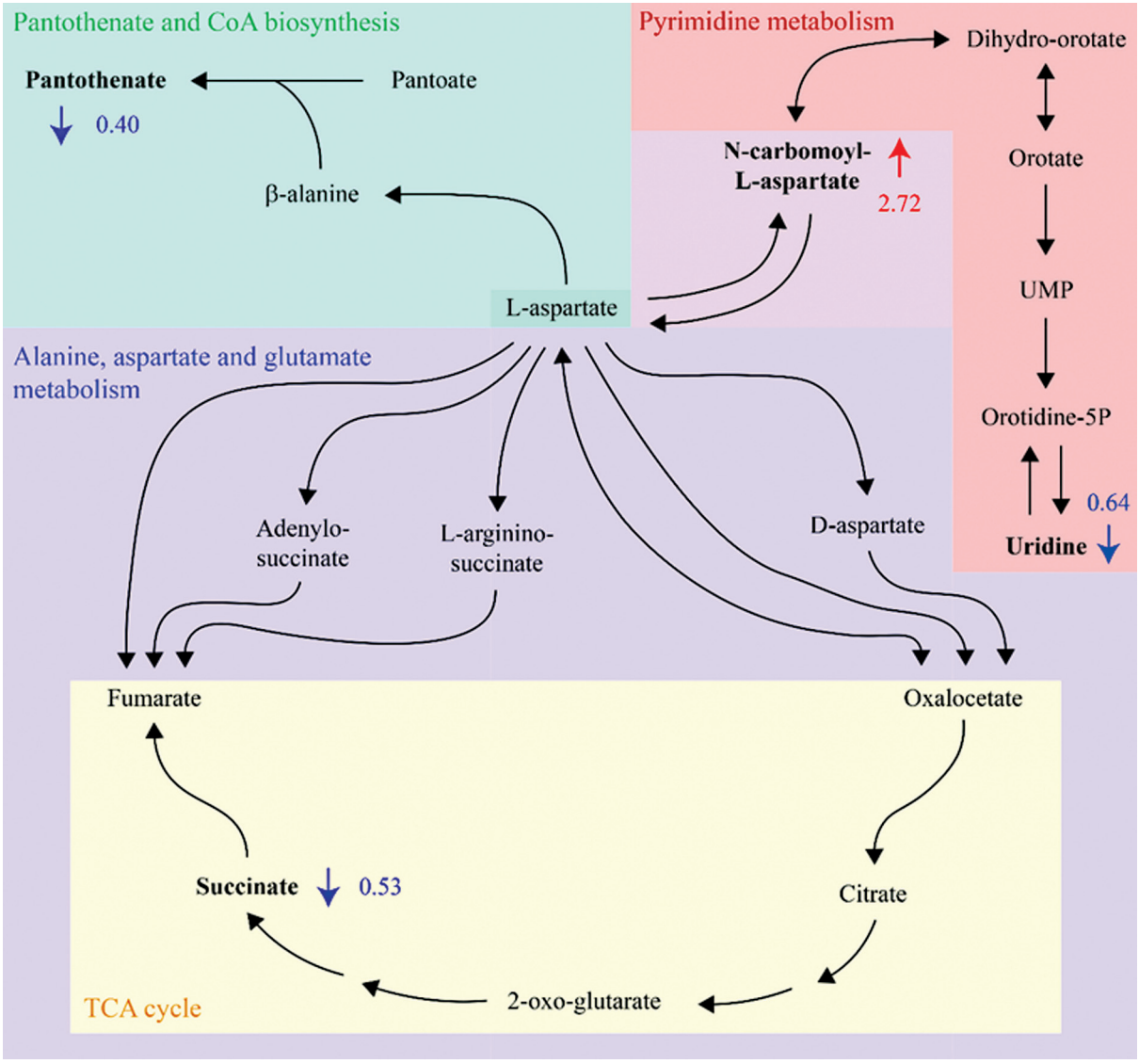

Fig. 4 *Metabolic alterations induced by GNYD treatment represented in an integrative metabolic network.* Significantly regulated metabolites are bolded, and the direction and magnitude of the fold change are denoted as arrows and value. Red and upwards arrows represent upregulated metabolites in the GNYD treatment group, whereas blue and downwards arrows represent downregulated metabolites in the GNYD treatment group.

immune cells,[25] and therapeutic targets for RA from the metabolic aspect have been proposed.[23]

In this study, the possible therapeutic mechanism of GNYD on RA was investigated. One of the metabolic pathways GNYD altered was the TCA cycle via the down-regulation of succinate. Succinic acid is metabolized by body cells and has a role in the tricarboxylic acid cycle as a cycle media component. It also functions as an inflammatory signaling molecule that is elevated in animals subjected to metabolic and inflammatory diseases by inducing IL-1β and HIF-1α.[26] In the context of RA, the induction of HIF-1α by succinic acid in turn leads to an induction of VEGF that will promote synovium angiogenesis.[27] It was also observed that the intra-articular microvascular blood flow has a high correlation with clinical synovitis in patients with RA,[28] further suggesting that angiogenesis plays a significant role in the disease progression of RA. Thus, the reduction of succinic acid and angiogenesis by GNYD in RA patients might be one possible mechanism of action.

Surprisingly, uridine in the pyridine metabolism pathway was found to be downregulated in the GNYD treatment group. One of the hallmarks of RA, hyperplasia of the synovial lining layer is caused by the excessive recruitment and accumulation of leukocytes in the synovium.[29,30] The recruited leukocytes, in turn, release pro-inflammatory cytokines that activate and stimulate the proliferation of resident synoviocytes.[31] Uridine was reported to have anti-inflammatory effects on an animal model of lung inflammation[32] as well as RA by suppressing extravasation of neutrophil, macrophage, and T cells into the synovium and inhibited synovial expression of intercellular adhesion molecule-1, CD-18, and cytokine production.[31] The results from this study suggest that GNYD has a component that is detrimental to RA, but this negative effect is less in magnitude than the

positive effect due to the reduction of angiogenesis. Further research can be done to identify the component that leads to the downregulation of uridine, and the efficacy of GNYD in treating RA with and without that particular component can then be compared. Besides uridine, N-carbamoyl-L-aspartate was found to be upregulated in this pathway as well. Since there was no significant correlation between N-carbamoyl-L-aspartate and uridine (►**Fig. 2B**), it suggests that the downregulation of uridine was independent of the change in N-carbamoyl-L-aspartate level.

Another metabolic pathway that was found to be significantly altered was the pantothenate and CoA biosynthesis pathway in which pantothenate was downregulated after treating with GNYD. Early research has shown that the level of pantothenate in RA patients was lower as compared with that in healthy people and the decrement of pantothenate level correlated with the severity of RA.[33] There exists weak evidence for the efficacy of pantothenate in treating RA whereby a 2 g daily intake of calcium pantothenate can reduce morning stiffness, pain, and disability of RA patients.[34] However, the above mentioned study utilized a small sample size. Without a further large scale, prospective study, the therapeutic link between pantothenate and RA remains a debatable manner. The results of this study do not seem to support this claim.

Some of the other significant regulated metabolites are reported to be related to anti-inflammation. For example, creatinine and anserine, both upregulated in the GNYD treatment group, are attributed to anti-inflammatory actions[35] with the latter being able to alleviate thioacetamide-induced fibrosis.[36] On the contrary, some anti-inflammatory agents were found to be reduced in the liver after GNYD treatment. One of these downregulated metabolites was thiamine. Thiamine deficiency can result in the impairment of oxidative metabolism, excitotoxicity, and inflammation in which the consequences include a series of events that set the stage for cerebral vulnerability.[37] Besides that, low circulation of pyridoxal was reported to be associated with the elevation of the inflammation marker C-reactive protein[38] and being a risk factor for inflammatory-related diseases including thrombosis and inflammatory bowel disease.[39] Gamma-L-glutamyl-L-valine exhibits antisepsis activity by reducing the expression of pro-inflammatory cytokines TNF-α, IL-6, and IL-1β in the plasma and small intestine as well as inhibiting the phosphorylation of the signaling proteins c-Jun N-terminal kinases (JNK) and nuclear factor-κB inhibitory factor α (IκBα) in a mouse model of LPS-induced sepsis.[40] This study prompts further research to be done on investigating the relationship between these metabolites and RA to elucidate the underlying complex network mechanism.

Conclusion

In conclusion, this study validated that GNYD treatment could regulate the metabolic profiles in the liver of hTNF-α transgenic arthritic model mice. GNYD can alter the TCA cycle and pyrimidine metabolism pathway via the regulation of succinic acid and uridine and affect the angiogenesis and leukocyte extravasation processes in RA. Further studies should be performed to illustrate the clear action mechanisms and explore other possible metabolic targets of RA.

Credit Authorship Contribution Statement

Yong Chen and Changhong Xiao: Concepting and designing the research. **Xingwang Zhu, Rongbin Pan and Wenting Zhao:** Carrying out the animal experiment and molecular studies, analysis and data curation. **Kok Suen Cheng:** Performing bioinformatics analysis of the study and writing original draft,and writing - review & editing.

Funding

This study was supported by the Scientific Research Project of Guangdong Province Traditional Chinese Medicine Bureau (20201229) and China Postdoctoral Science Foundation Project (2021M701438).

Conflict of Interest

The authors declare no conflict of interest.

References

1 McInnes IB, Schett G. Pathogenetic insights from the treatment of rheumatoid arthritis. Lancet 2017;389(10086):2328–2337
2 Burmester GR, Pope JE. Novel treatment strategies in rheumatoid arthritis. Lancet 2017;389(10086):2338–2348
3 Lo LC, Chen CY, Chiang JY, Cheng TL, Lin HJ, Chang HH. Tongue diagnosis of traditional Chinese medicine for rheumatoid arthritis. Afr J Tradit Complement Altern Med 2013;10(05):360–369
4 Zukow W, Kalisz Z, Muszkieta R, et al. Acupuncture for rheumatoid arthritis: a randomized, sham-controlled clinical trial. J Acupunct Tuina Sci 2011;9(03):168–172
5 Zhang P, Li J, Han Y, Yu XW, Qin L. Traditional Chinese medicine in the treatment of rheumatoid arthritis: a general review. Rheumatol Int 2010;30(06):713–718
6 Chen Y, Luo D, Cai JF, et al. Effectiveness and safety of glycyrrhizae decoction for purging stomach-fire in Behcet disease patients: study protocol for a randomized controlled and double-blinding trail. Medicine (Baltimore) 2018;97(13):e0265
7 Zhu S, Sugiyama R, Batkhuu J, Sanchir C, Zou K, Komatsu K. Survey of Glycyrrhizae radix resources in Mongolia: chemical assessment of the underground part of Glycyrrhiza uralensis and comparison with Chinese glycyrrhizea radix. J Nat Med 2009;63(02):137–146
8 Hofseth LJ, Wargovich MJ. Inflammation, cancer, and targets of ginseng. J Nutr 2007;137(1, Suppl):183S–185S
9 Grzanna R, Lindmark L, Frondoza CG. Ginger—an herbal medicinal product with broad anti-inflammatory actions. J Med Food 2005;8(02):125–132
10 Conte C, Epstein S, Napoli N. Insulin resistance and bone: a biological partnership. Acta Diabetol 2018;55(04):305–314
11 Arias de la Rosa I, Escudero-Contreras A, Rodríguez-Cuenca S, et al. Defective glucose and lipid metabolism in rheumatoid arthritis is determined by chronic inflammation in metabolic tissues. J Intern Med 2018;284(01):61–77
12 Rempenault C, Combe B, Barnetche T, et al. Metabolic and cardiovascular benefits of hydroxychloroquine in patients with rheumatoid arthritis: a systematic review and meta-analysis. Ann Rheum Dis 2018;77(01):98–103
13 Li G, Wu Y, Jia H, et al. Establishment and evaluation of a transgenic mouse model of arthritis induced by overexpressing human tumor necrosis factor alpha. Biol Open 2016;5(04):418–423

14 Vigerust NF, Bjørndal B, Bohov P, Brattelid T, Svardal A, Berge RK. Krill oil versus fish oil in modulation of inflammation and lipid metabolism in mice transgenic for TNF-α. Eur J Nutr 2013;52(04): 1315–1325
15 Wei R, Wang J, Su M, et al. Missing value imputation approach for mass spectrometry-based metabolomics data. Sci Rep 2018;8 (01):663
16 Dunn WB, Broadhurst D, Begley P, et al.Human Serum Metabolome (HUSERMET) Consortium. Procedures for large-scale metabolic profiling of serum and plasma using gas chromatography and liquid chromatography coupled to mass spectrometry. Nat Protoc 2011;6(07):1060–1083
17 Xu XH, Wang C, Li SX, et al. Friend or foe: differential responses of rice to invasion by mutualistic or pathogenic fungi revealed by RNAseq and metabolite profiling. Sci Rep 2015;5:13624
18 Xia J, Wishart DS. MetPA: a web-based metabolomics tool for pathway analysis and visualization. Bioinformatics 2010;26(18): 2342–2344
19 Triba MN, Le Moyec L, Amathieu R, et al. PLS/OPLS models in metabolomics: the impact of permutation of dataset rows on the K-fold cross-validation quality parameters. Mol Biosyst 2015;11(01):13–19
20 Qiu Y, Zhou B, Su M, et al. Mass spectrometry-based quantitative metabolomics revealed a distinct lipid profile in breast cancer patients. Int J Mol Sci 2013;14(04):8047–8061
21 Li C, Liu X, Wang H, Fan H, Chen Y. Koumiss consumption induced changes in the fecal metabolomes of chronic atrophic gastritis patients. J Funct Foods 2019;62:103522
22 Zheng M, Qin Q, Zhou W, et al. Metabolic disturbance in hippocampus and liver of mice: a primary response to imidacloprid exposure. Sci Rep 2020;10(01):5713
23 Falconer J, Murphy AN, Young SP, et al. Review: synovial cell metabolism and chronic inflammation in rheumatoid arthritis. [J] Arthritis Rheumatol 2018;70(07):984–999
24 Metsios GS, Stavropoulos-Kalinoglou A, Nevill AM, Douglas KM, Koutedakis Y, Kitas GD. Cigarette smoking significantly increases basal metabolic rate in patients with rheumatoid arthritis. Ann Rheum Dis 2008;67(01):70–73
25 Xu C, Wang W, Zhong J, et al. Canagliflozin exerts anti-inflammatory effects by inhibiting intracellular glucose metabolism and promoting autophagy in immune cells. Biochem Pharmacol 2018;152:45–59
26 Tannahill GM, Curtis AM, Adamik J, et al. Succinate is an inflammatory signal that induces IL-1β through HIF-1α. Nature 2013; 496(7444):238–242
27 Li Y, Liu Y, Wang C, et al. Succinate induces synovial angiogenesis in rheumatoid arthritis through metabolic remodeling and HIF-1α/VEGF axis. Free Radic Biol Med 2018;126:1–14
28 Strunk J, Heinemann E, Neeck G, Schmidt KL, Lange U. A new approach to studying angiogenesis in rheumatoid arthritis by means of power Doppler ultrasonography and measurement of serum vascular endothelial growth factor. Rheumatology (Oxford) 2004;43(12):1480–1483
29 Guo Q, Wang Y, Xu D, Nossent J, Pavlos NJ, Xu J. Rheumatoid arthritis: pathological mechanisms and modern pharmacologic therapies. Bone Res 2018;6:15
30 Mellado M, Martínez-Muñoz L, Cascio G, Lucas P, Pablos JL, Rodríguez-Frade JM. T cell migration in rheumatoid arthritis. Front Immunol 2015;6:384
31 Chenna Narendra S, Chalise JP, Magnusson M, Uppugunduri S. Local but not systemic administration of uridine prevents development of antigen-induced arthritis. PLoS One 2015;10(10): e0141863
32 Evaldsson C, Rydén I, Uppugunduri S. Anti-inflammatory effects of exogenous uridine in an animal model of lung inflammation. Int Immunopharmacol 2007;7(08):1025–1032
33 Barton-Wright EC, Elliott WA. The pantothenic acid metabolism of rheumatoid arthritis. Lancet 1963;2(7313):862–863
34 Wheatley D. Calcium pantothenate in arthritic conditions. A report from the General Practitioner Research Group. Practitioner 1980;224(1340):208–211
35 Madan BR, Khanna NK. Effect of creatinine on various experimentally induced inflammatory models. Indian J Physiol Pharmacol 1979;23(01):1–7
36 Chen PJ, Tseng JK, Lin YL, et al. Protective effects of functional chicken liver hydrolysates against liver fibrogenesis: antioxidation, anti-inflammation, and antifibrosis. J Agric Food Chem 2017;65(24):4961–4969
37 Hazell AS, Butterworth RF. Update of cell damage mechanisms in thiamine deficiency: focus on oxidative stress, excitotoxicity and inflammation. Alcohol 2009;44(02):141–147
38 Friso S, Jacques PF, Wilson PW, Rosenberg IH, Selhub J. Low circulating vitamin B(6) is associated with elevation of the inflammation marker C-reactive protein independently of plasma homocysteine levels. Circulation 2001;103(23): 2788–2791
39 Saibeni S, Cattaneo M, Vecchi M, et al. Low vitamin B(6) plasma levels, a risk factor for thrombosis, in inflammatory bowel disease: role of inflammation and correlation with acute phase reactants. Am J Gastroenterol 2003;98(01):112–117
40 Chee ME, Majumder K, Mine Y. Intervention of dietary dipeptide gamma-l-glutamyl-l-valine (γ-EV) ameliorates inflammatory response in a mouse model of LPS-induced sepsis. J Agric Food Chem 2017;65(29):5953–5960